Iranian Journal of Science & Technology, Transaction A, Vol. 34, No. A2
Printed in the Islamic Republic of Iran, 2010

ELECTRONIC AND STRUCTURAL PROPERTIES OF TIN DIOXIDE IN CUBIC PHASE*

H. SALEHI, M. ARYADOUST** AND M. FARBOD

Department of Physics, Shahid Chamran University, Ahvaz, I. R. of Iran
Email: aryadoustm@yahoo.com

Abstract – The electronic structure, energy band structure and electronic density of SnO_2 ceramic in cubic phase have been investigated using first principle full potential-linearized augmented plane wave (FP-LAPW) method within density functional theory (DFT). Local density approximation (LDA) and the generalized gradient approximation (GGA), which are based on exchange- correlation energy optimization were used. The band gap was 2.2 eV at Γ point in the Brillouin zone within our approach. Calculations of the band structure and electronic structure of SnO_2 were in a good agreement with the previous experimental and theoretical results with different approximations. Moreover, electronic density map shows that the bonding between Sn and O atoms is ionic.

Keywords – Lattice constant, bulk module, ceramic SnO_2, electronic structure, electronic density distribution

1. INTRODUCTION

Tin dioxide (SnO_2) is an n-type broad-band gap (3.6eV) oxide semiconductor with high chemical and mechanical stabilities [1]. SnO_2, which has outstanding optical, electrical and mechanical properties, is a versatile material and has wide usage as the most attractive material for gas sensor applications [2] as a catalyst during the oxidation of organic compounds, as a key component in rechargeable Li batteries and as a master element in opto-electronic devices [3].

Thin films of SnO_2 possess very interesting physical properties [4-8] such as high electrical conductivity coupled with fairly large optical transmission in a visible region. Owing to its low resistivity and high transmittance, SnO_2 thin films are used as window layers and heat reflectors in solar cells [9, 10], various gas sensors [11], flat panel displays, electro-chromic devices, invisible security circuits, LEDs and etc. Now, SnO_2 thin films have been become an integral part of modern electronic technology.

2. THE METHOD OF CALCULATION

The calculations are performed using the scalar relativistic FP-LAPW approach as implemented in WIEN2K code within the framework of density functional theory (DFT), which has been shown to yield reliable results for the electronic structural properties of various solids. For structural properties the exchange- correlation potential was calculated using both the local density approximation (LDA) and the generalized gradient approximation (GGA) in the form proposed by Perdew et al. [12-15]. The initial lattice constant ($a=4.925\,\overset{0}{A}$) was provided from experimental results [16]. In this calculation, the convergence parameter is $Rk_{max}=7$ and the other parameters are $G_{max}=14$, RMT (Sn) = 2.1au, RMT (O) = 1.7 au. We used 20×20×20 meshes which generated 1767 k-points in the first Brillion zone.

*Received by the editor August 31, 2009 and in final revised form October 6, 2010
**Corresponding author

3. RESULTS AND DISCUSSION

a). Band structure

The calculated energy-band structure for SnO_2 in cubic phase at the high symmetry direction in the Brillouin zone is shown in Fig. 1. In this approach, the numbers generated are 1767 k-points and the convergence parameter, choose Rk_{max}=7 and the convergence is stabilized in terms of energy. The distinction between the valence and core state is made through the value of energy, thus the value of -6 Ry is taken as the boundary separating the core electron states from the valence electron states. Table 1 shows the number of core states for atoms in SnO_2, six orbital for Sn atoms and two orbital for O atoms.

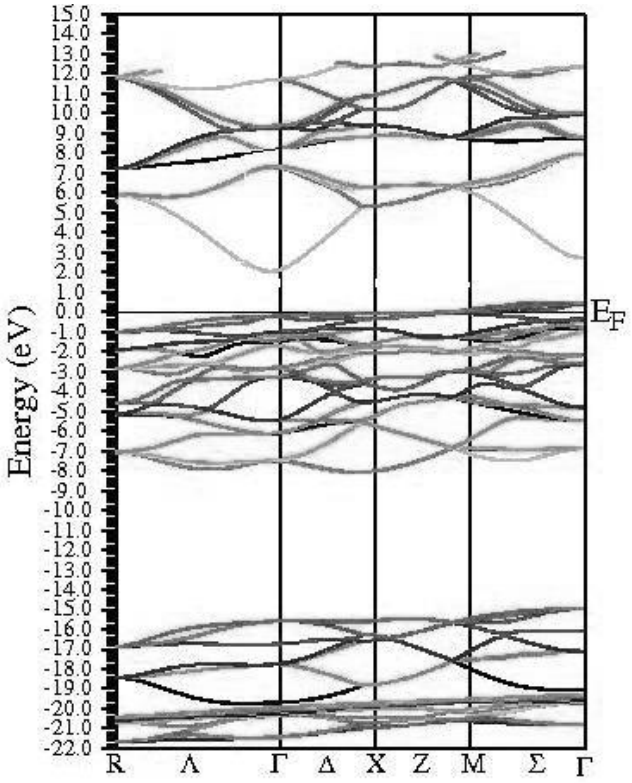

Fig. 1. Band structure for cubic SnO_2

Table 1. Total schematic of core, semi core and valance states for SnO_2

atom	Core	semi core	valance
Sn	$1s^2,2s^2,2p^6,3s^2,3p^6,3d^{10}$	$4s^2,4p^6,4d^{10}$	$5s^2,5p^2$
O	$1s^2$	$2s^2$	$2p^4$

The band gap is 2.2 eV at Γ point in the Brillouin zone within our approach. The energy band gaps obtained from SnO_2 are given in Table 2. The values are compared with previous studies. It has been seen that our results agree favorably with past results [17].

Table 2. Energy band gap (eV) in this work and compared with other results for cubic SnO_2

	Present work			Other work
	FP-LAPWGGA96	FP-LAPW GGA91	FP-LAPW LDA	Theoretical results[17]
Γ	2.2	2	1.7	0.5

The conduction bands arise from s and p such as states of the Sn atom with their bottom located at the Γ point in the cubic phase. The lowest lying bands shown in Fig. 1 arise from the Oxygen s states. The upper valence bands that lie above these bands are mainly due to Sn and Oxygen P states.

b) Electronic structures

In this work, the structural parameters of SnO_2 were obtained by calculating the total energy at various value of the lattice parameters around the experimental values. This was carried out within the FP-LAPW method with the GGA and LDA scheme without the spin orbits coupling effects, by fitting the Murnaghan equation of state to the total energies versus lattice parameter (a), the bulk modulus B and pressure derivative of bulk modulus B′, which are compared with previous theoretical and experimental studies in Table 3. Here, present results for SnO_2 are compared with previous experimental and theoretical results. The detailed behavior of the energy as a function of the cubic volume is shown in Fig. 2. The theoretical lattice constant and bulk modulus in this section are obtained through fitting the total energy data with the Murnaghan of state [18].

$$E(V) = E_0 + \frac{B_0 V_0}{B'}\left[\frac{V}{V_0} + \frac{\left(\frac{V}{V_0}\right)^{1-B'} - B'}{B'-1}\right] \quad (1)$$

where E(v) is the DFT ground state energy with the cell volume V, V_0 is the unit cell volume at zero pressure, B denotes the bulk modulus, and its first derivative with respect to the pressure is $B_0' = \partial B / \partial P$ at P=0.

Table 3 shows that, in this way the calculated parameters are fairly similar to the experimental data. On the other hand, compressibility is defined by the inverse of bulk module. The bulk modulus shows the hardness of the crystal. As the bulk modulus increases, consequently the crystal hardness will increase.

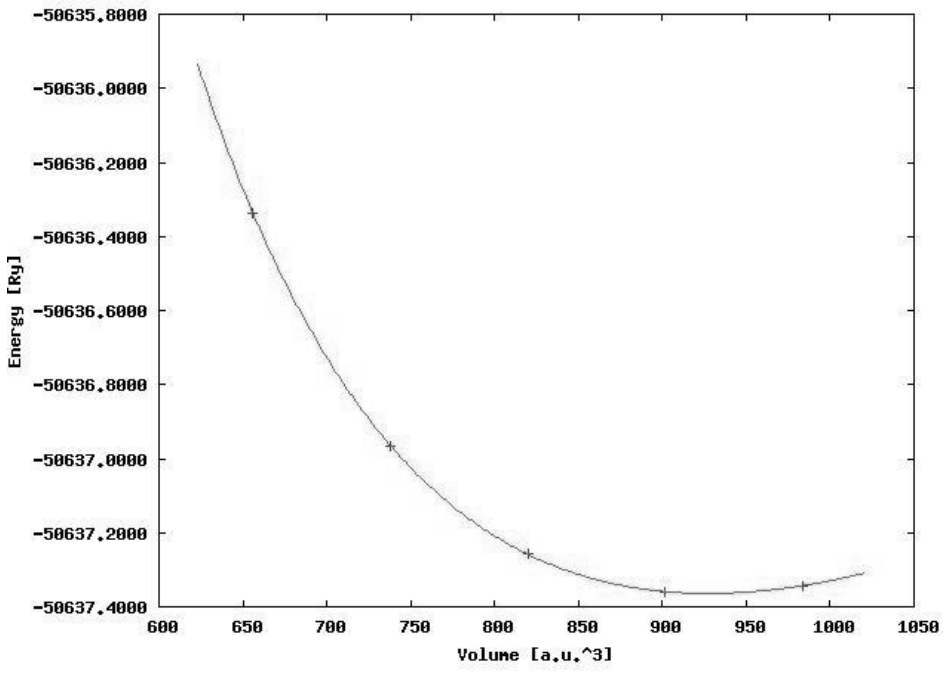

Fig. 2. Total energy function of the volume for cubic SnO_2

Table 3. The calculation structure parameters in this work and compared with other results for cubic SnO_2

Present work				Other calculated values	
Quantity	FP-LAPW GGA96	FP-LAPW GGA91	FP-LAPW LDA	Experimental result	Theoretical result
$a\ (A^0)$	5.1561	5.1567	5.0693	4.9526 [16]	5.079 [17]
Difference with exp.(%)	4.10%	4.12%	2.35%	0%	2.49%
B(Gpa)	201.2581	201.7674	204.8333	-	213 [17]
B'	3.1043	3.0973	6.5253	-	-
K(Gpa)	4.9687×10^{-3}	4.9562×10^{-3}	4.8820×10^{-3}	$4.8076\ [17]\times10^{-3}$	-

The results show a cubic symmetric. Pressure effects can be isotropic in all directions and with an increase in the pressure, the cell volume decreases. Now, we are discussing the pressure effect on the SnO_2 structure. First, the dependence of the volume to the pressure can be obtained from equation 1, then by differentiation of this equation, whit respect to the volume and by using the thermodynamic equation dE=-PdV, one can obtain:

$$V(P) = V_0\left[(\frac{B'}{B})P + 1\right]^{\frac{-1}{B'}}. \qquad (2)$$

Figure 3 shows the dependence of the volume to the pressure within interval (1-30) GPa for SnO_2 in the cubic structure. This diagram indicated that, by increasing the pressure, the unit cell volume decreases. The small variation of volume to interval (1-30) GPa shows a low condensation and a high hardness from SnO_2.

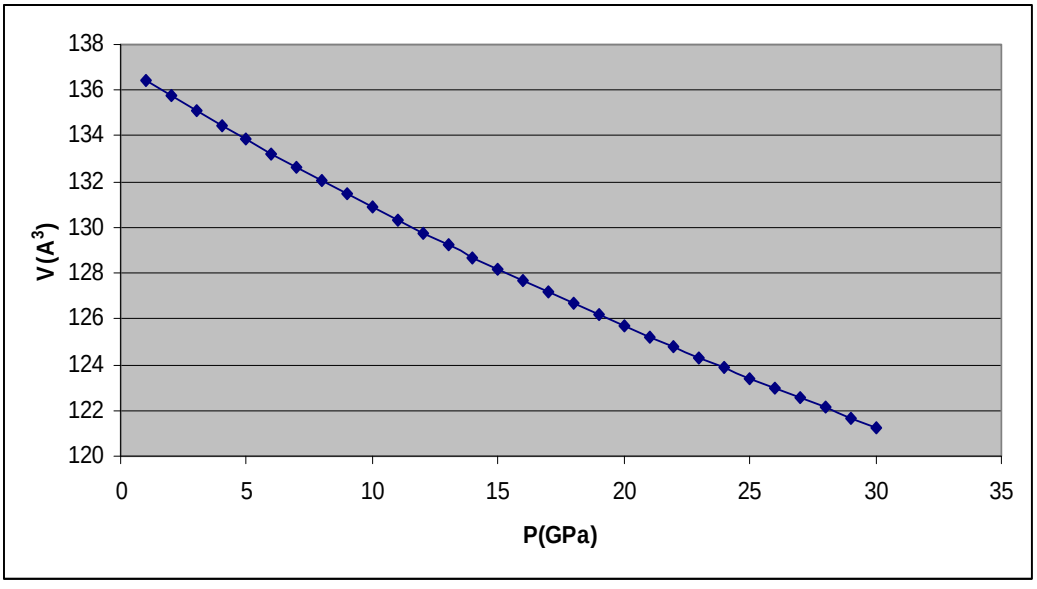

Fig. 3. Changes of cell volume for composite SnO_2 in cubic phase with respect to pressure

c) The condensation of SnO_2 crystal

Condensation of volume is obtained by equation:

$$K_V = -\frac{1}{V_0}\frac{dV}{dP} \tag{3}$$

where V_0 is the equilibrium volume at zero pressure and volume magnitude replaced from Table 2. The gradient of curve 3 was computed, and then condensation of the volume was calculated. In fact, condensation is inversing the bulk modulus and has an inverse relation with hardness. Magnitude of volume condensation and high bulk modulus indicated that SnO_2 ceramic has a hard body and necessitates high energy for metamorphosis in crystal SnO_2. Furthermore, linear condensation has been obtained in the direction of axes by equation:

$$K_r = -\frac{V_0}{B_0}\frac{d\ln(r)}{dV} \tag{4}$$

where r, V_0 and B_0 are lattice constant, equilibrium volume and bulk modulus at zero pressure respectively. At first, we have plotted the curve with respect to equilibrium volume in Fig. 4, then the gradient was computed from this diagram and $d\ln(a)/dV$ was obtained from this gradient. In Table 4 the computed linear condensation in the direction of axes is shown.

Table 4. Compressibility of volume and linear for SnO_2 crystal in cubic phase

compressibility	FP-LAPWLDA
$K_V\ (Gpa)^{-1}$	4.8820×10^{-3}
$K_a\ (Gpa)^{-1}$	1.714×10^{-3}

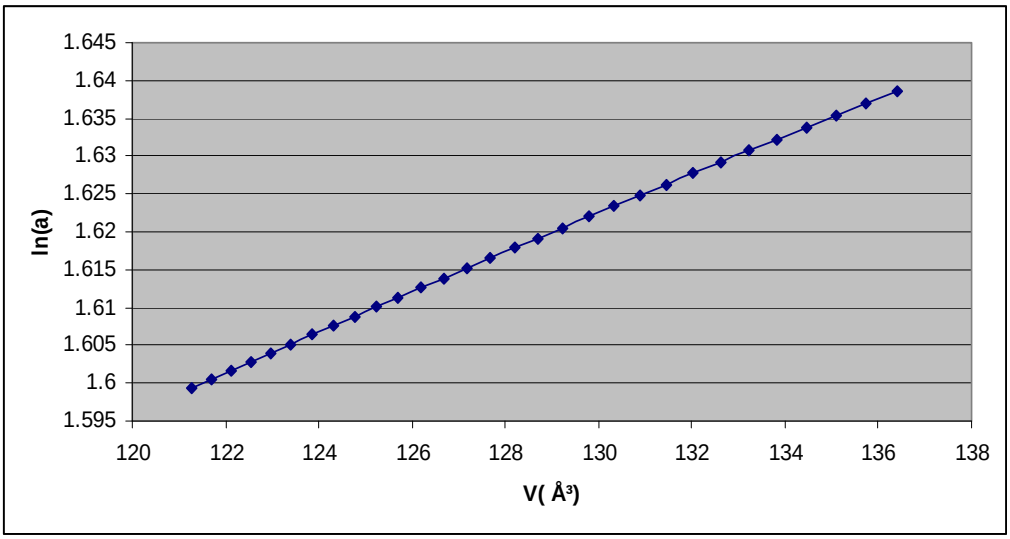

Fig. 4. Changes of lna for SnO_2 in cubic phase with respect to equilibrium volume

Tables 5 and 6 show some information about the electric charge in the muffin-tin spheres for Sn and O atoms. They indicate that the muffin-tin sphere's radius selections are the best. Calculations show that the nearest distance between Sn and O atoms does not depend on the kind of approximation, but only on the lattice constant. These distances are the same for all states that are calculated with the theoretical constant and the experimental constant. One of the parameters which is interesting for studying the structural properties of a compound is the effective charge. The amount of this charge and the amount of inequality from an atom's nominal charge is one reason for an ionic joint being in the compound. The

calculated effective charge for SnO_2 atoms are given in table 7 in different approximations and they are compared with nominal charges.

According to the result in Table 7, in this composite there are 0.5194 electrons for each tin atom and 1.6732 electrons for each O atom. So, the ionic formula for this composite in the cubic phase is suggested, such as $Sn^{0.5194}\ O^{1.6732}$. The inequality formula from nominal formula SnO_2 shows that there are ionic bonds between atoms in this compound. Table 7 indicates that the effective charges on the Sn and O atoms are very close to the values of the ionic charge.

Table 5. Charge decomposition for Sn atom in SnO_2

Approximate	FP-LAPWGGA96	FP-LAPWGGA91	FP-LAPWLDA	FP-LAPWLSDA
Nominal charge	50	50	50	50
Charge of inside sphere muffin-tin	46.79541	46.798461	46.85402	46.97405
Core charge	35.97182	35.92538	35.97201	36.06919
Valance charge	10.823559	10.87308	10.88201	10.90486
Charge of outside sphere muffin-tin	3.20513	3.202079	3.14652	3.0 2606
Sum of inside and outside sphere muffin-tin charge	50.00054	50.00054	50.00054	50.00007

Table 6. Charge decomposition for O atom in SnO_2

Approximate	FP-LAPWGGA96	FP-LAPWGGA91	FP-LAPWLDA	FP-LAPWLSDA
Nominal charge	8	8	8	8
Charge of inside sphere muffin-tin	6.65926	6.86545	6.6450	7.05555
Core charge	1.390043	1.285051	1.072247	1.647872
Valance charge	5.269217	5.580399	5.572753	5.407678
Charge of outside sphere muffin-tin	1.34076	1.1348	1.35462	1.45091
Sum of inside and outside sphere muffin-tin charge	8.00002	8.00002	8.00002	8.50646

Table 7. Effective charge calculated in this work compared other results for cubic SnO_2

Approximate	FP-LAPWGGA96	FP-LAPW GGA91	FP-LAPW LDA	FP-LAPW LSDA	Formula charge
O	1.6614	1.6812	1.7 590	1.5932	2
Sn	0.4905	0.5 230	0.5 317	0.5 323	1

d) Electronic charge density

The bonding nature of the solids can be described accurately by using electronic density plots that have been calculated in the content of first principles approach. The charge density in our work is derived from a high-converged wave function, hence the result is very reliable and it can then be used to study the bonding nature of the solid. The charge density distribution was calculated and the difference in density plot between the crystalline and superposed atomic densities for SnO_2 compound at equilibrium volume of cubic structure in the (1 1 0) plane, as shown in Fig. 5. Visual comparison of the corresponding charge density plots show that the bonding nature of these compounds is mainly ionic, leading to the strong localization of charge the anion.

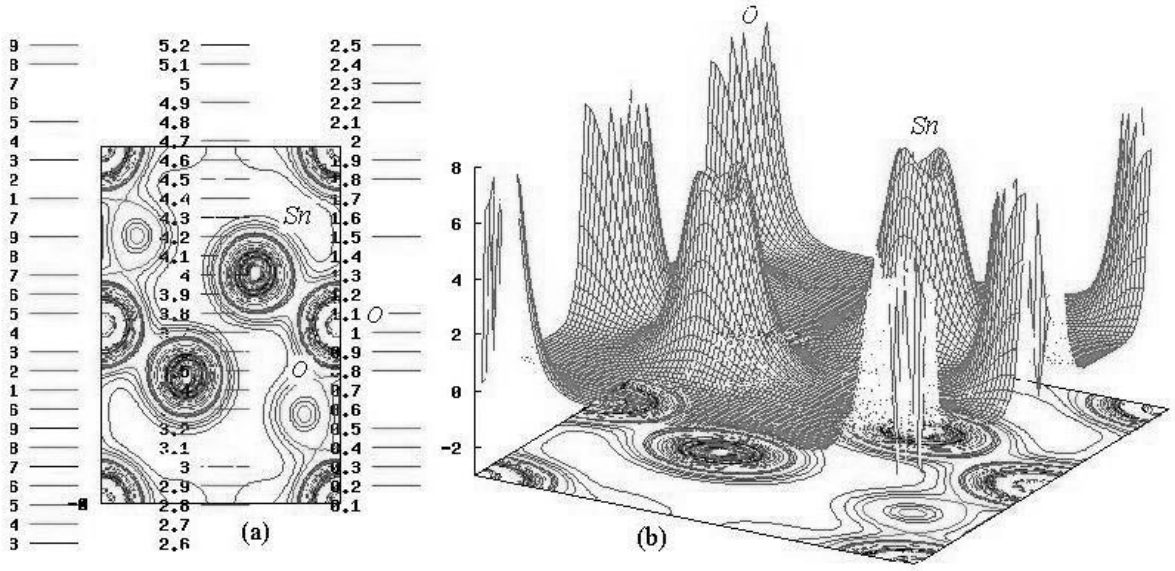

Fig. 5. Electron density distribution for cubic phase of SnO_2 in the (110) plane
(a) in two dimensions and (b) in three dimensions

4. CONCLUSION

We have applied a FP-LAPW method to study the structural and electronic properties of SnO_2 compound. The scalar relativistic approach was adopted for the valence state, whereas the core states are treated fully relativistically. The results are summarized as follows:

i) We have calculated the equilibrium lattice parameter, bulk modulus, pressure derivative of bulk modulus B′ and energy band gap SnO_2. The obtained results show that SnO_2 has a direct band gap.

ii) From the magnitude of volume condensation and high bulk module one can conclude that SnO_2 ceramic has a hard body and high energy is necessary for metamorphosis in SnO_2 crystal.

iii) The bonding character has been discussed as a strong localization of charge around the anion. Our calculation predicated the ionic bonding for this compound. Results also show that the charge distribution and the nature of the chemical bonding are in good agreement with the previous experimental and theoretical works [16, 17].

REFERENCES

1. Toupance, T., Babot, O., Jousseaume, B. & Villaca, G. (2003). Anocrystalline Mesoporous Tin Dioxide Prepared by the Sol−Gel Route from a Dialkoxydi (β-Diketonato) tin Complex. *chem. Mater.*, *15*(24), 4691-4697.
2. Vuong, D. D., Sakai, G., Shimanoe, K. & Yamazoe, N. (2004). Preparation of grain size-controlled tin oxide sols by hydrothermal treatment for thin film sensor application. *Sens. Actuators, B*103, 386-391.
3. Velasques, C., Jas, F. R, Ojedagortiz, M. L. & Campero, A. (2005). Structure and texture of self-assembled nanoporous SnO_2. *Nanothecnology, 16*, 1278-1284.
4. Sevik, C. & Bulutay, C. (2006). High-dielectric constant and wide band gap inverse silver oxide phases of the ordered ternary alloys of SiO_2, GeO_2 and SnO_2. *phy. Rev.*, *B*74, 193201.
5. Vasu, V. & Subrahmanyan, A. (1991). Physical properties of sprayed SnO_2 films. *Thin Solid Films*, *202*(2) 283-288.
6. Bhagavat, G. K. & Sundram, K. B. (1979). Electrical and photovoltaic properties of tin oxide-silicon heterojunctions. *Thin Solid Films*, *63*(1) 197-201.

7. Elangovan, E. & Ramamurthi, K. (2003). Studies on optical properties of polycrystalline SnO_2: Sb thin films prepared using $SnCl_2$ precursor. *Cryst. Res. Technol*., *38*, 779.
8. Dobler, D., Oswald, S., Behr, G., Werner, J. & Wetzig, K. (2003). Changes of Auger parameter in doped SnO_2 powders. *Cryst. Res. Technol*., *38*, 956.
9. Matthias, B. & Diebold, U. (2005). The surface and materials science of tin oxide. *Progress in Surface Science, 79*, 47-154.
10. Supachai, N., Thammanoon, S., Yoshikazu, S. & Susumu, Y. (2006). Doubled layered ITO/ SnO_2 conducting glass for substrate of dye-sensitized solar cells. *Solar Energy Materials and Solar Cells*, *90*, 2129.
11. Nomura, K., Ujihira, Y., Sharma, S. S., Fueda, A. & Murakami, T. (1989). Gas sensitivity of metal oxide mixed tin oxide films prepared by spray pyrolysis. *J. Mater. Sci., 24*, 937-941.
12. Hohenberg, P. & Kohn, W. (1964). Inhomogeneous Electron Gas. *Phys. Rev*. *136*B, 864-871.
13. Kohn, W. & Sham, L. J. (1965). Self-Consistent Equations Including Exchange and Correlation Effects. *Phys. Rev. A, 140*, 1133-1138.
14. Perdew, J. P., Burke, K. & Ernzerhof, M. (1996). Generalized Gradient Approximation Made Simple. *Phys. Rev. Lett., 77*(18), 3865-3868.
15. Schwarz, K., Blaha, P. & Madsen, G. K. H. (2002). Electronic structure calculations of solids using the WIEN2k package for material sciences. *Comput. Phys. Commun., 147*(1-2), 71-76.
16. Haines, J. & Léger, J. M. (1997). X-ray diffraction study of the phase transitions and structural evolution of tin dioxide at high pressure: Relationships between structure types and implications for other rutile-type dioxides. *Phys. Rev., B55*(17), 11144-11154.
17. El Haj Hassan, F., Alaeddine, A., Zoaeter, M. & Rachidi, I. (2005). First-Principles Investigation of SnO_2 at High Pressure. *International Journal of Modern Physics B, 19*(27), 4081-4092.
18. Murnaghan, F. D. (1944). The Compressibility of Media under Extreme Pressures. *Proc. Natl. Acad. Sci.* (244-247). USA.